Biogeosciences Discuss., 10, 9989–10019, 2013
www.biogeosciences-discuss.net/10/9989/2013/
doi:10.5194/bgd-10-9989-2013

Biogeosciences Discussions
Open Access

The photobleaching as a factor controlling spectral characteristics of chromophoric dissolved organic matter in open ocean

Y. Yamashita[1,2], Y. Nosaka[2], K. Suzuki[1,2], H. Ogawa[3], K. Takahashi[4], and H. Saito[5]

[1]Faculty of Environmental and Earth Science, Hokkaido University, N10, W5, Kita-ku, Sapporo, Hokkaido 060-0810, Japan
[2]Graduate School of Environmental Science, Hokkaido University, N10, W5, Kita-ku, Sapporo, Hokkaido 060-0810, Japan
[3]Atmosphere and Ocean Research Institute, The University of Tokyo, 5-1-5, Kashiwanoha, Kashiwa-shi, Chiba 277-8564, Japan
[4]Graduate School of Agricultural and Life Sciences, The University of Tokyo, 1-1-1, Yayoi, Bunkyo-ku, Tokyo, 113-8657, Japan
[5]Tohoku National Fisheries Research Institute, Fisheries Research Agency, 3-27-5 Shinhama-cho, Shiogama 985-0001, Japan

Received: 10 May 2013 – Accepted: 22 May 2013 – Published: 19 June 2013

Correspondence to: Y. Yamashita (yamashiy@ees.hokudai.ac.jp)

Published by Copernicus Publications on behalf of the European Geosciences Union.

Abstract

Chromophoric dissolved organic matter (CDOM) ubiquitously occurs in marine environments and plays a significant role in the marine biogeochemical cycles. Basin scale distributions of CDOM have recently been surveyed in the global ocean and indicate that quantity and quality of oceanic CDOM are mainly controlled by in situ production and photo-degradation. However, factors controlling the spectral parameters of CDOM at UV region, i.e., spectral slope of CDOM determined at 275–295 nm ($S_{275–295}$) and the ratio of two spectral slope parameters (S_R; the ratio of $S_{275–295}$ to $S_{350–400}$), have not been well documented. To evaluate the factor controlling the spectral characteristics of CDOM at UV region in open ocean, we determined the quantitative and qualitative characteristics of CDOM in the subarctic and subtropical surface waters (5–300 m) of the western North Pacific. Absorption coefficients at 320 nm in the subarctic region were significantly higher than those in the subtropical region throughout surface waters, suggesting that magnitudes of photobleaching were different between the two regions. The values of $S_{275–295}$ and S_R were also significantly higher in the subtropical region than the subarctic region. The dark microbial incubation showed biodegradation of DOM little affected $S_{275–295}$, but slightly decreased S_R. On the other hand, increases and unchanging were observed for $S_{275–295}$ and S_R during photo-irradiation incubations respectively. These experimental results indicated that photobleaching of CDOM mainly induced qualitative differences in CDOM at UV region between the subarctic and subtropical surface waters. The results of this study imply that $S_{275–295}$ can be used as a tracer of photochemical history of CDOM in open ocean.

1 Introduction

Chromophoric dissolved organic matter (CDOM) ubiquitously occurs in open ocean (Kitidis et al., 2006; Nelson et al., 2007, 2010; Swan et al., 2009; Yamashita and Tanoue, 2009). It has known that CDOM is one of the major factors controlling optical proper-

BGD
10, 9989–10019, 2013

ties of seawater (Siegel et al., 2002; Nelson and Siegel, 2013), and thus, to be controlling the light penetration, especially, in the UV region (Fichot et al., 2008; Nelson and Siegel, 2013) which affects the primary, microbial production, and also the structure of marine food web (Smith et al., 1992; Herndl et al., 1993; Häder et al., 1998). CDOM has also known to be an important player in biogeochemical cycles since it is highly photo-reactive and is destroyed upon exposure to sunlight, producing inorganic carbon, volatile species such as carbonyl sulfide, and bioavailable low molecular weight DOM (Mopper and Kieber, 2002).

The distributions of CDOM in coastal environments are strongly controlled by riverine inputs of terrestrial (allochthonous) CDOM (Blough and Del Vecchio, 2002). However, major fraction of CDOM in open ocean has been considered to be produced autochthonously through various biological processes (Nelson et al., 2004; Steinberg et al., 2004; Ortega-Retuerta et al., 2009; Shank et al., 2010), and the primary local source of CDOM has been assigned to be related to microbial activity (Nelson et al., 2004; Yamashita and Tanoue, 2004). From the global distribution of CDOM, microbially produced CDOM has been considered as biologically refractory components with the time scale of the thermohaline circulation (Nelson et al., 2007, 2010; Yamashita and Tanoue, 2008; Swan et al., 2009), and thus, CDOM has been suggested as a tracer of deep ocean biogeochemical processes and circulation (Nelson et al., 2007, 2010). As such, the distribution of CDOM in open ocean is basically controlled by a balance between autochthonous production and photobleaching under the influence of transport by vertical mixing, ventilation, and upwelling of water masses.

The chemical composition of CDOM in open ocean estimated with the spectral slope parameter (S) has known to be different among sources (Kitidis et al., 2006; Yamashita and Tanoue, 2009). S has also known to change with photobleaching (Swan et al., 2012) or diagenesis (Nelson et al., 2007) of CDOM. These imply that S can be used as a tracer of sources and/or biogeochemical history of CDOM in open ocean. However, lack of standard method to determine the S limits its usefulness since its value depends on the wavelength range for estimation (Carder et al., 1989; Stedmon et al.,

BGD
10, 9989–10019, 2013

2000; Twardowski et al., 2004). Recently, the ratio of the spectral slope parameters (S_R) obtained from two wavelength ranges, i.e., S at 275 nm to 295 nm ($S_{275–295}$) to 350 to 400 nm ($S_{350–400}$), was introduced as the indices of molecular weight of DOM and photobleaching history (Helms et al., 2008). The S_R has been widely applied to evaluating the environmental dynamics of DOM in terrestrial aquatic environments (e.g, Yamashita et al., 2010a,b; Osburn et al., 2011; Mladenov et al., 2011) as well as coastal environments (Guéguen et al., 2011; Shank and Evans, 2011; Romera-Castillo et al., 2013). In addition, $S_{275–295}$ was successfully used as a retrieve method of DOC concentration and as a tracer of terrestrial DOC in river-influenced ocean margin (Fichot and Benner, 2011, 2012; Fichot et al., 2013). Since $S_{275–295}$ can be measured with high precision due to relatively high absorbance levels in this wavelength range (Helms et al., 2008), these spectral parameters may also be used as a tracer of water masses and biogeochemical history of CDOM in open ocean where CDOM levels are quite low (Nelson et al., 2007, 2010; Swan et al., 2009; Yamashita and Tanoue, 2009). However, even the distribution of these parameters has not been evaluated in open ocean.

Since the levels of CDOM in open ocean is basically controlled by microbial production, photobleaching, and transport as mentioned above, the levels of CDOM in the surface water is higher in subpolar regions compared with subtropical regions due to extensive photobleaching of CDOM at subtropical regions (Nelson et al., 2007, 2010; Swan et al., 2009; Yamashita and Tanoue, 2009). Thus, it can be hypothesized that S_R and $S_{275–295}$ in the subpolar surface water are significantly different from those in the subtropical surface water due to different photobleaching history of CDOM, and thus, these parameters can be used as biogeochemical tracers in open ocean. In this study, we determined the spectral characteristics of CDOM, including S_R and $S_{275–295}$, in surface waters (~ 300 m) of the subarctic and the subtropical regions at the northwestern North Pacific. In addition, in order to examine S_R and $S_{275–295}$ as a potential biogeochemical tracer, the changes in CDOM spectral characteristics along with photobleaching of CDOM and microbial degradation of DOM were evaluated.

BGD
10, 9989–10019, 2013

2 Materials and methods

2.1 Observation and sample collection

Sampling locations are shown in Fig. 1. Samplings of the subarctic region were carried out at 2 stations (SA-A-1, SA-A-2) on 20 April 2010 by the R/V *Wakataka-maru* (WK1004), at 2 stations (SA-J-1, SA-J-2) from 9 to 11 June 2010 by the R/V *Wakataka-maru* (WK1006), and at 2 stations (SA-M-1, SA-M-2) from 10 to 11 May 2011 by the R/V *Tansei-maru* (KT-11-07). Samplings of the subtropical region were carried out at 3 stations (ST-1, ST-2, ST-3) from 19–20 May 2010 during the R/V *Hakuhou-maru* cruise (KH-10-01).

Seawater samples for CDOM analyses were collected from 5 m to 300 m at the above mentioned 9 stations with a CTD carousel system equipped with Niskin bottles. The plastic in-line filter holder that contained pre-combusted (450 °C, 3–5 h) glass fiber filter (GF/F) was attached directly to the spigot of Niskin bottle, and seawater was gravity filtered into pre-combusted glass vial with teflon-lined cap after triple rinsing. The samples were then stored frozen in the dark until analysis. All the equipment except glassware were pre-soaked in 5–10 % HCl and rinsed thoroughly with Milli-Q water.

Chlorophyll *a* (Chl *a*) concentrations were determined using two methods. For samples form the subarctic region, high-performance liquid chromatography (HPLC) was used following Endo et al. (2013). Chl *a* concentrations at the subtropical region were determined by the fluorometric method of Welshmeyer (1994).

2.2 Microbial incubation experiments

To evaluating the changes in CDOM quantity and quality during microbial degradation of bioavailable DOM, seawater bottle incubation experiments were performed according to Hasegawa et al. (2010). Seawater samples were collected from 5 m at two stations in the subarctic region on 10 May 2011 during the KT-11-07 cruise (Table 1). Seawater was gravity filtered using GF/F filter into pre-cleaned 20 L polycarbonate bot-

BGD
10, 9989–10019, 2013

tle after triple rinsing, and the filtrate was then dispensed into 24 pre-combusted glass bottles with teflon-coated caps after triple rinsing. Half of glass bottles containing the GF/F filtrate were incubated under the dark at the room temperature (16–25 °C) and others were incubated under the dark in the refrigerator (1–6 °C) that were close to surface seawater temperature (Table 1). Triplicate samples for each treatment were sequentially collected at 10, 20, and 40 days from a set of experimental bottles and filtered using pre-combusted GF/F filter, and then, stored frozen in the dark until analysis.

2.3 Photo-irradiation experiments

Seawater samples were collected from 400 m and 766 m at the subtropical region (Fig. 1, Table 1) on 19 November 2012 during the cruise of R/V *Tansei-maru* (KT-12-31). The large surface area 0.2 µm capsule filter (HCl pre-cleaned AcroPak, Pall) was attached directly to the spigot of Niskin bottle, and seawater was gravity filtered into pre-cleaned 9 L polycarbonate bottle after triple rinsing. The filtrate was kept in the dark at ~ 4 °C until photo-irradiation experiments conducted on land. Eighteen 50 mL quartz bottles were filled with the filtered seawater sample after triple rinsing. Then, 9 out of the 18 bottles were wrapped with aluminum foil. The quartz bottles containing the filtrate were incubated in the water bath on the roof of the Environmental Science building, Hokkaido University (43.1° N, 141.3° E) under natural sunlight for 13 days. The water bath maintained a temperature between 3 and 10 °C through the irradiation during daytime, and the quartz bottles were kept in the refrigerator (~ 4 °C) during nighttime. On the days of 2, 6, and 13 during incubation, three replicate samples for each treatment were allowed to stand in the dark until reaching near room temperature (approx. 23 °C), and then, absorbance analyses were carried out without further filtration. The global solar radiation was measured by a pyranometer (SR507, Field Pro) installed on the roof of the Environmental Science building. The cumulative irradiance was 23, 60, and 87 MJ m^{-2} for 2, 6, and 13 days, respectively.

BGD
10, 9989–10019, 2013

2.4 Absorbance measurements

Water samples were thawed and allowed to stand until reaching room temperature (approx. 23 °C) prior to absorbance measurements. Absorbance spectra were obtained between 200 and 1000 nm at 0.5 nm intervals using a spectrophotometer (UV-1800, Shimadzu) equipped with 10 cm or 5 cm quartz-windowed cells. Absorbance spectra of a blank (Milli-Q) and samples were obtained against air, and a blank spectrum was subtracted from each sample spectrum. Sample spectrum was baseline-corrected by subtracting average values ranging from 590 to 600 nm from the entire spectrum (Yamashita and Tanoue, 2009), and then converted to absorption coefficients, $a(\lambda)$ (m^{-1}) (Green and Blough, 1994). CDOM absorption spectra are declining exponentially with wavelength (Fig. 2) and have usually been fit to an exponential function as follows (Green and Blough, 1994):

$$a(\lambda) = a(\lambda_i)e^{-S(\lambda-\lambda_i)}$$

where $a(\lambda)$ and $a(\lambda_i)$ are the absorption coefficients at wavelength λ and reference wavelength λ_i (m^{-1}), respectively. S is the spectral slope parameter (nm^{-1}). The absorption coefficient at 320 nm, $a(320)$, was reported as a quantitative parameter of CDOM (Yamashita and Tanoue, 2009). The S_R value, the ratio of the S obtained from the two regions, 275 nm to 295 nm ($S_{275–295}$) and 350 to 400 nm ($S_{350–400}$), was calculated according to Helms et al. (2008).

3 Results

3.1 Vertical profiles of salinity, temperature, and Chl *a*

Salinity ranges in the upper 300 m water column of the subarctic region were 32.9–33.7, 32.9–33.8, and 32.9–33.7 in April, May, and June, respectively (Fig. 3). Temperature ranged from 2.4 to 4.5 °C in April, 2.0 to 4.7 °C in May, and 0.6 to 9.0 °C in June.

BGD
10, 9989–10019, 2013

These water masses could be categorized as a cold subarctic Oyashio water according to the criterion of a temperature of < 5 °C at a depth of 100 m (Kawai, 1972). Chl *a* concentrations were significantly different among the sampling periods, i.e., ~ 8.8 μg L^{-1} in April, ~ 2.3 μg L^{-1} in May, and ~ 0.7 μg L^{-1} in June. From the Chl *a* concentration, April, May, and June could be categorized as spring bloom, decline of the bloom, and post bloom phase, respectively (Saito et al., 2002).

Salinity and temperature at 3 stations of the subtropical region ranged from 34.7 to 35.0 and 16.6 to 26.4 °C, respectively. The highest temperature and salinity were evident in the upper 150 m waters at ST-3 most closely located to the central part of the subtropical gyre. Chl *a* concentrations at the subtropical region were quite low (less than 0.6 μg L^{-1}) compared to the subarctic region and showed subsurface maxima at 74, 70 and 114 m at ST-1, ST-2, and ST-3, respectively.

3.2 Vertical profiles of CDOM quantity and quantity

Levels of CDOM were higher in the subarctic region compared with the subtropical region (Fig. 2). *a*(320), ranged from 0.253 to 0.372 m^{-1} in the subarctic region and from 0.056 to 0.159 m^{-1} in the subtropical region (Fig. 4). The values of *a*(320) in each region were similar with those in the subarctic and subtropical surface waters of the central North Pacific, respectively (Yamashita and Tanoue, 2009) and were similar with or slightly higher than *a*(325) in the surface waters of the Pacific (Swan et al., 2009). In the subarctic region, the levels of *a*(320) and Chl *a* in the upper water column (~ 50 m) were higher than those in the lower water column irrespective of differences in sampling periods. However, the temporal change in *a*(320) in the upper water column did not accompany with that in Chl *a* concentration in the Oyashio waters. The lowest value of *a*(320) in this study was found at ST-3 in the subtropical region. At ST-3, *a*(320) tended to increase with depth. The levels of *a*(320) at ST-1 and ST-2 showed subsurface maxima at 50 m which were shallower than the subsurface Chl *a* maxima.

Figure 2b shows typical absorption spectrum on logarithmic scale at the subarctic and subtropical regions. At the wavelengths shorter than 300 nm, the decline of ab-

BGD
10, 9989–10019, 2013

sorption spectrum with wavelength was steeper for the subtropical region than the subarctic region. Values of $S_{275–295}$ were high at the subtropical region (0.0339–0.0556 nm^{-1}), especially upper 100 m at ST-3, compared with the subarctic region (0.0203–0.0330 nm^{-1}) but decreased with depth, irrespective of difference in oceanic regions (Fig. 4). The values of $S_{275–295}$ at the subarctic region were similar irrespective of difference in sampling periods. The range of $S_{275–295}$ observed in this study was higher than those in river waters (Helms et al., 2008; Spencer et al., 2012), but $S_{275–295}$ in the subarctic waters and the subtropical waters were similar to those found in the Hudson Bay and Hudson Strait (Guéguen et al., 2011) and in the high salinity Gulf of Mexico waters (Fichot and Benner, 2012), respectively.

$S_{350–400}$ tended to decrease as depth increased irrespective of difference in oceanic regions, and the values were not different between the subarctic and subtropical regions. The ranges of $S_{350–400}$ (0.0114 to 0.0174 for all samples) found in this study were relatively smaller than those found in river waters (Helms et al., 2008; Spencer et al., 2012), but were similar with those found in the high salinity Gulf of Mexico waters (Fichot and Benner, 2012).

Significant difference in S_R, basically due to difference in $S_{275–295}$, was also evident between the subarctic and the subtropical waters. Interestingly, vertical profiles of S_R in the subarctic region showed small subsurface maxima at depths between 30 and 80 m. Vertical profiles of S_R did not show any clear increase or decrease trends among 3 stations in the subtropical region. The range of S_R found in the subarctic waters (1.61–2.12) was generally higher than that in the river waters (Helms et al., 2008; Yamashita et al., 2010a, b; Spencer et al., 2012). The S_R in the subtropical waters ranged from 2.48 to 4.05. These values were similar to that found for the Georgia Bight but smaller than that found for the Sargasso Sea (Helms et al., 2008).

3.3 Changes in CDOM during dark microbial incubations

Figure 5 shows the changes in CDOM quantity and quality during dark microbial incubation. Hasegawa et al. (2010) conducted similar experiments for 15 to 38 days us-

BGD
10, 9989–10019, 2013

ing GF/F filtrate of Oyashio waters collected during pre-bloom, bloom, and post-bloom phases and found that 2.1–8.3 % of initial DOC was consumed by bacteria. Thus, the microbial degradation of DOM could occur during the dark microbial incubations in this study. Even though different temperatures, i.e., room and cool temperatures, were used for dark microbial incubations, differences in quantitative and qualitative parameters of CDOM during incubations were not clear between them. The levels of CDOM, $a(320)$, decreased with time during incubations at the cool temperature. The decrease in $a(320)$ during the SAM-2 cool incubation was larger than that of the SAM-1 cool incubation. At the room temperature, $a(320)$ sharply decreased for first 10 days, then did not change over the SAM-2 room incubation, on the other hand, $a(320)$ sharply increased for first 10 days, and then decreased from 10 to 40 days for the SAM-1 room incubation. Such changes in CDOM quantity during dark incubations could be explained by the combination of degradation of bioavailable fraction and microbial production (Nelson et al., 2004; Biers et al., 2007). The magnitudes of change in $a(320)$ ($\sim 0.067\,m^{-1}$) during 40 days incubations were comparable to its spatial and temporal differences observed in the surface waters of the subarctic region (Fig. 4).

$S_{275–295}$ did not change systematically during incubations. Compared with the initial values ($d = 0$), the changes in $S_{275–295}$ were less than $0.0011\,nm^{-1}$ during 40 days incubations with one exception ($0.0027\,nm^{-1}$ for SAM-1 room at 10 days). The magnitudes of change in $S_{275–295}$ during dark incubations were quite small compared with the ranges observed for vertical differences ($\sim 0.01\,nm^{-1}$ at the subarctic region, $\sim 0.02\,nm^{-1}$ at the subtropical region, Fig. 4). On the other hand, $S_{350–400}$ increased throughout the incubations with increment of $0.0012–0.0018\,nm^{-1}$ for 40 days. The net increments in $S_{350–400}$ during incubation were comparable to those found for vertical differences in the subtropical and the subarctic regions (Fig. 4). As a result of changes in $S_{275–295}$ and $S_{350–400}$, S_R continued to decrease during incubations. The net decrements of S_R during 40 days incubations (0.15–0.26) were similar with vertical differences found in the subarctic region (Fig. 4).

BGD
10, 9989–10019, 2013

3.4 Changes in CDOM during photo-irradiation experiments

Levels of $a(320)$ were significantly decreased for light treatments but not for dark experiments during photo-irradiation experiments (Fig. 6), indicating the photobleaching of CDOM during natural sunlight irradiation. The net decreases in $a(320)$ were 0.068 and 0.081 for STP-1 and STP-2 light experiments, respectively. Such magnitudes of decrease in $a(320)$ for 13 days photo-irradiation were comparable to its spatial and temporal differences found in the surface waters of the subarctic region (Fig. 4). During the photobleaching of CDOM, $S_{275–295}$ continued to increase with the increment of 0.0093 and 0.0067 nm^{-1} for 13 days STP-1 and STP-2 light experiments, respectively. It should be noted that this range was one order of magnitude greater than that found during 40 days dark microbial incubations. On the other hand, the values of $S_{275–295}$ were constant throughout the experiments for STP-1 and STP-2 dark experiments. $S_{350–400}$ also tended to increase with increment of 0.0027–0.0039 for 13 days during photobleaching of CDOM, even though the values were largely scattered among the three replicates. $S_{350–400}$ at dark treatments also tended to increase for 13 days experiments, implying that increases in $S_{350–400}$ observed during photobleaching of CDOM might be overestimated. As a result, S_R did not change with large variation for the three replicates throughout the photo-irradiation experiments.

4 Discussion

4.1 Factors controlling the CDOM level at the subarctic and the subtropical region

The accumulation of DOC along with phytoplankton bloom events has been observed for the Oyashio waters of the subarctic region (Hasegawa et al., 2010). On the other hand, the levels of CDOM, namely $a(320)$, in the subarctic region did not change significantly along with phytoplankton bloom events, i.e., bloom (April), the decline of bloom

BGD
10, 9989–10019, 2013

(May), and post bloom (June) phases, indicating that major factors controlling the bulk DOM and CDOM levels are different and phytoplankton is not major source of CDOM in this study area (Figs. 3 and 4). At the BATS site in the Sargasso Sea, seasonal cycle of CDOM level has been considered as results of photobleaching, winter convective mixing, and production during heterotrophic recycling of organic carbon rather than primary production (Nelson et al., 1998; Nelson and Siegel, 2002). The microbial production of CDOM has also been observed during microbial culture experiments (Nelson et al., 2004; Biers et al., 2007; Ortega-Retuerta et al., 2009). On the other hand, various biological sources, i.e., zooplankton (Steinberg et al., 2004; Ortega-Retuerta et al., 2009), cyanobacteria *Trichodesmium* spp. (Steinberg et al., 2004), dinoflagellates (Vernet and Whitehead, 1996), have been considered as sources of CDOM. The CDOM derived from such specific sources usually have distinct peak in absorbance spectra. In the present study, distinct peaks were not evident in CDOM spectra (Fig. 2). In addition, spectral slope parameters, i.e., $S_{275–295}$, $S_{350–400}$, and S_R, were not significantly different among sampling periods in the subarctic region, suggesting that heterotrophic microbial regeneration, rather than phytoplankton and zooplankton activity, seems to be major source of CDOM for the Oyashio waters at the subarctic region.

The higher levels of CDOM in the upper 50 m waters compared with 50–300 m waters were possibly due to higher microbial production. Kobari et al. (2010) reported that bacterial abundance and growth were not related to Chl *a* concentration during the spring phytoplankton bloom events in the Oyashio region. The active regeneration with high bacterial production was observed after the peak of primary production during in situ iron enrichment experiments conducted at the subarctic region of the northwestern North Pacific (Kudo et al., 2009). However, in the present study, highest levels of CDOM did not occur during the decline of bloom (May) or post bloom (June) phases. Such temporal pattern of CDOM level suggests that degradation of newly produced CDOM is an important factor controlling the CDOM level in the Oyashio waters at the subarctic region. The photobleaching that causes decrease in CDOM level occurs with time scale of hours to days (Fig. 6; Swan et al., 2012). The microbial culture incubation

BGD
10, 9989–10019, 2013

experiments have highlighted the production of a bioavailable CDOM fraction that is quickly degraded by microbes within days (Nelson et al., 2004; Biers et al., 2007). Our dark microbial incubation experiments also showed net decrease in CDOM with one exception (Fig. 5). These pieces of evidence suggested that major fractions of newly produced CDOM might disappear rapidly due to the photobleaching and/or microbial degradation. Interestingly, subsurface maxima of CDOM level were clearly observed for 20–30 m at SA-J-1 and SA-J-2 (Fig. 4), suggesting whether photobleaching dominated in surface waters (< 20 m) or freshly produced CDOM accumulated in the subsurface layer (20–30 m) during the post bloom phase.

The levels of CDOM in the subtropical region were significantly lower than those in the subarctic region throughout the water column (Fig. 4). Such difference in CDOM level (subarctic > subtropical) have also been found for basin scale observations of CDOM (Kitidis et al., 2006; Nelson et al., 2007, 2010; Swan et al., 2009; Yamashita and Tanoue, 2009) as well as satellite observations of CDOM (e.g., Siegel et al., 2002; Bricaud et al., 2012). Low levels of CDOM in the lower water column due to contribution of mode water have also been observed in subtropical regions (Nelson et al., 2007, 2010; Yamashita and Tanoue, 2009; Swan et al., 2009). The low levels of CDOM found in the subtropical region has been explained by extensive photobleaching of CDOM due to the long residence time of surface waters in the subtropical gyres with high solar insolation (Swan et al., 2009). Seasonal variability of vertical profiles and chemical characteristics of fluorescent DOM in the subtropical region of the western Pacific were also explained by deep winter mixed layer and the extensive photobleaching (Omori et al., 2010, 2011). Thus, different levels of CDOM found between the subarctic and the subtropical regions in this study can be explained mainly by differences in photobleaching degree of CDOM between the regions.

Subsurface maxima of CDOM level were found at ST-1 and ST-2 in the subtropical region (Fig. 4). These maxima are possibly due to the results of photobleaching and microbial production of CDOM as discussed above. On the other hands, at the southern most ST-3, lowest level of CDOM, possibly due to extensive photobleaching, was found

BGD
10, 9989–10019, 2013

in the surface water (5–10 m) and the CDOM level increased with depth below the surface water. It should be noted that ST-3 is closely located to the central part of the subtropical gyre, consequently, the upper water column at ST-3 is relatively stratified throughout a year compared with ST-1 and ST-2. In addition, the upper water column at ST-3 characterized as high salinity suggests longer exposure to sunlight in the sea surface. Interestingly, the levels of CDOM in the waters deeper than 150 m were similar among three stations, suggesting that the same water mass was distributed for 150–300 m at the 3 stations.

4.2 Spectral characteristic of CDOM as a biogeochemical tracer in open ocean

In analogy with difference in CDOM quantity due to different degree of photobleaching, some of qualitative parameters of CDOM also showed significant differences between the subarctic and the subtropical regions (Fig. 4). The values of $S_{275–295}$ were significantly different between the subarctic and the subtropical regions. Such difference in $S_{275–295}$ between two oceanic regions was consistent with the results of photo-irradiation experiments, i.e., increase in $S_{275–295}$ along with photobleaching of CDOM (Fig. 6). In addition, lowest level of CDOM found at ST-3, possibly due to extensive photobleaching, was accompanied with the highest $S_{275–295}$. Even though changes in $S_{275–295}$ during photo-irradiation experiments using oceanic DOM have scarcely been reported, increase in $S_{275–295}$ was also observed during photo-irradiation experiment of the North Atlantic Deep Water (Stubbins et al., 2012). Ortega-Returerta et al. (2010) conducted the photo-irradiation incubations using Southern Ocean waters and found that $S_{275–295}$ exhibited a net increase over the incubation where photobleaching was the dominant process, whereas that did not show this trend in the incubations where photohumification (photo-induced transformation) was observed. Increases in $S_{275–295}$ have also been observed during photobleaching of terrestrial and coastal DOM (Helms et al., 2008; Zhang et al., 2009b; Osburn et al., 2011; Fichot and Benner, 2012). From the relationships between $S_{275–295}$ and salinity observed at the northern Gulf of Mexico,

BGD
10, 9989–10019, 2013

Fichot and Benner (2012) suggested that photobleaching is a major process regulating $S_{275–295}$ in surface waters regardless of origin, i.e., marine or terrigenous.

It appears $S_{275–295}$ changed slightly but did not exhibit systematic increase/decrease trend during dark microbial incubation (Fig. 5). The slight decrease in $S_{275–295}$ was found during microbial incubation of river water (Helms et al., 2008). Fichot and Benner (2012) found the slight decrease in $S_{275–295}$ (1–2.4 %) during microbial incubation of ambient coastal DOM. They also conducted the microbial incubation experiments of ambient coastal DOM (that $S_{275–295}$ values were 0.0168–0.0196 nm^{-1}) with addition of protein-rich plankton DOM obtained from a diatom bloom (that $S_{275–295}$ was 0.0259 nm^{-1}) and found that $S_{275–295}$ decreased moderately with degradation of highly labile, protein-rich plankton DOM. These experimental results suggest that $S_{275–295}$ is not change significantly by microbial degradation (modification) of bioavailable DOM, even though highly labile, protein-rich DOM shows relatively high $S_{275–295}$ values. Therefore, in conclusion, $S_{275–295}$ can be used as a tracer of photochemical history of CDOM in open ocean.

The increase in $S_{275–295}$ during photobleaching of terrestrial and coastal CDOM has been considered as the result of destroy of high molecular weight CDOM into low molecular weight CDOM (Helmes et al., 2008). This increase, however, could also be explained by the solar radiation spectrum and absorption spectra of CDOM. Del Vecchio and Blough (2002) found that the primary (direct) loss of CDOM absorption occurred at the irradiation wavelength, with smaller secondary (indirect) losses occurring outside the irradiation wavelength using monochromatic radiation. Using polychromatic radiation that is comparable to solar radiation, they also found that the relative loss of CDOM absorption was greater at longer wavelengths due to (1) the greater photons at longer wavelengths and (2) the higher rates of indirect absorption loss at longer wavelengths. Fichot and Benner (2012) pointed out that $S_{275–295}$ increase with greater indirect loss of absorption at 295 nm compared to 275 nm during irradiation under the natural solar radiation, because the position of 275–295 nm window is the outer edge of the incident solar spectrum. In fact, Swan et al. (2009) estimated the absorbed quanta

BGD
10, 9989–10019, 2013

by CDOM (Q_a) that was calculated by solar simulator spectrum and oceanic CDOM absorption spectra and found that Q_a was sharply increased from 300 nm, peaked at 320–325 nm, then gradually decreased toward 450 nm. Such spectral characteristics of solar radiation and CDOM cause less photobleaching at the shorter wavelength region, and thus, increase in $S_{275–295}$ during photobleaching of CDOM.

The significant difference between the subarctic and the subtropical regions was also found for S_R, implying that high S_R values found at the subtropical waters were results of photobleaching of CDOM (Fig. 4). The S_R values, on the other hand, did not increase along with photobleaching of CDOM during photo-irradiation experiments (Fig. 6), even though increases in S_R were found during photo-irradiation of terrestrial and coastal CDOM (Helms et al., 2008). $S_{350–400}$ tended to increase accompanied with increase in $S_{275–295}$ during photobleaching of CDOM, resulting the unchanged S_R values in this study (Fig. 6). Zhang et al. (2009b) reported the decrease in $S_{350–400}$ during photobleaching of lake CDOM. On the other hand, Osburn et al. (2011) found the slight increase in $S_{350–400}$ during photobleaching of lake CDOM. The different behavior, i.e., increase or decrease trend, of $S_{350–400}$ among samples submitted to photo-irradiation was also found (Helms et al., 2008). These results suggest that changes in $S_{350–400}$ during photobleaching of CDOM might depend on CDOM sources that related to chemical compositions. $S_{350–400}$ were not different significantly between the subarctic and the subtropical regions (Fig. 4). Such spatial characteristics of $S_{350–400}$ imply that an important factor controlling the $S_{350–400}$ value is not photobleaching of CDOM in open ocean. In addition, Swan et al. (2012) found the photobleaching of CDOM absorption at 300–360 nm with simultaneous increases in the absorption at 360–500 nm for samples from high-nutrient low-chlorophyll regions. Thus, S_R calculated by $S_{275–295}$ and $S_{350–400}$ can not be used as a tracer of photochemical history of CDOM in open ocean.

Interestingly, S_R showed subsurface maxima in the subarctic region, suggesting that newly produced CDOM has higher S_R values and/or S_R values changed during microbial degradation processes of CDOM. In our dark microbial incubation experiments, decreases in S_R due to increase in $S_{350–400}$ were evident along with degradation of

BGD
10, 9989–10019, 2013

bioavailable oceanic CDOM (Fig. 5). This result implies that S_R might be useful as a tracer of microbial reworking history of oceanic CDOM. Helms et al. (2008), on the other hand, found the decrease in S_R due to decrease in the $S_{275–295}$ and increase in the $S_{350–400}$ for degradation of terrigenous DOM. Zhang et al. (2009a) reported the increase, and then, decrease trend of S_R during lake phytoplankton degradation experiment. Such different trend of S_R during DOM degradation might be results of differences in sources, i.e., terrigenous or autochthonous. Further study is needed for evaluating the S_R as well as $S_{350–400}$ as a tracer of photochemical and/or microbial reworking history in relation to sources of CDOM.

5 Conclusions and perspectives

This study demonstrated that photobleaching is primary factor controlling the $S_{275–295}$ in surface waters of the northwestern North Pacific. The results are consistent with previous studies conducted in terrestrial aquatic environments as well as coastal environments (Helmes et al., 2008; Fichot and Benner, 2012). Thus, like as terrestrial and costal environments, $S_{275–295}$ can be used as a possible tracer for photochemical history of CDOM in open ocean. Helms et al. (2008) pointed out that $S_{275–295}$ may be used for tracing subducted, photobleached surface water. In this study, we discussed possible contribution of the same water mass into the lower water column at 3 stations in the subtropical region from the distributional pattern of $S_{275–295}$. The subsurface and intermediate waters such as mode waters have intrinsic formation regions (e.g., Suga et al., 2004) where photochemical histories of CDOM are possibly different. Thus, $S_{275–295}$ can be used for evaluating the distribution of mode waters. In addition, $S_{275–295}$ can also be used for tracing the episodic upwelling events caused by such as tropical cyclones. The vertical transport of photo-labile CDOM from subsurface into surface waters might affect the primary and microbial production because photo-degradation of CDOM gives rise the microbiologically labile low molecular weight compounds (Mopper and Kieber, 2002). To clarify this issue, effects of photo-degradation of CDOM with

BGD
10, 9989–10019, 2013

changes in $S_{275–295}$ on the biological production should be evaluated. CDOM at visible region has often been focused, because CDOM in this region can be determined, in other words, it is important factor estimating the accurate chlorophyll concentration by satellite remote sensing (e.g., Sasaki et al., 2004; Matsuoka et al., 2007). Since $S_{275–295}$ can be measured with high precision and give rise useful information for marine biogeochemistry, inclusion of this analysis in future optical studies in open ocean is highly expected.

Acknowledgements. We are grateful to K. Sugie, and captains and crews of the R/V *Wakataka-maru*, the R/V *Tansei-maru*, the R/V *Hakuho-maru* for their assistance with sample collection. This research was supported by grants-in-aid from JSPS (No. 22840002, 23651003, and 24681002 to Y.Y.; 24121003 to H.S.).

References

Biers, E. J., Zepp, R. G., and Moran, M. A.: The role of nitrogen in chromophoric and fluorescent dissolved organic matter formation, Mar. Chem., 103, 46–60, 2007.

Blough, N. L. and Del Vecchio, R.: Chromophoric DOM in the coastal environment, in: Biogeochemistry of Marine Dissolved Organic Matter, edited by: Carlson, C. and Hansell, D., Academic Press, 509–546, 2002.

Bricaud, A., Ciotti, A. M., and Gentili, B.: Spatial-temporal variations in phytoplankton size and colored detrital matter absorption at global and regional scales, as derived from twelve years of SeaWiFS data (1998–2009), Global Biogeochem. Cy., 26, GB1010, doi:10.1029/2010GB003952, 2012.

Carder, K. L., Steward, R. G., Harvey, G. R., and Ortner, P. B.: Marine humic and fulvic acids: their effects on remote sensing of ocean chlorophyll, Limnol. Oceanogr., 34, 68–81, 1989.

Del Vecchio, R. and Blough, N. V.: Photobleaching of chromophoric dissolved organic matter in natural waters: kinetics and modeling, Mar. Chem., 78, 231–253, 2002.

Endo, H., Yoshimura, T., Kataoka, T., and Suzuki, K.: Effects of CO_2 and iron availability on phytoplankton and eubacterial community compositions in the northwest subarctic Pacific, J. Exp. Mar. Biol. Ecol., 439, 160–175, 2013.

BGD
10, 9989–10019, 2013

Fichot, C. G. and Benner, R.: A novel method to estimate DOC concentrations from CDOM absorption coefficients in coastal waters, Geophys. Res. Lett., 38, L03610, doi:10.1029/2010GL046152, 2011.
Fichot, C. G. and Benner, R.: The spectral slope coefficient of chromophoric dissolved organic matter ($S_{275-295}$) as a tracer of terrigenous dissolved organic carbon in river-influenced ocean margins, Limnol. Oceanogr., 57, 1453–1466, 2012.
Fichot, C. G., Sathyendranath, S., and Miller, W. L.: SeaUV and SeaUVC: algorithms for the retrieval of UV/Visible diffuse attenuation coefficients from ocean color, Remote Sens. Environ., 112, 1584–1602, 2008.
Fichot, C. G., Kaiser, K., Hooker, S. B., Amon, R. M. W., Babin, M., Bélanger, S., Walker, S. A., and Benner, R.: Pan-Arctic distributions of continental runoff in the Arctic Ocean, Sci. Rep., 3, 1053, doi:10.1038/srep01053, 2013.
Green, S. A. and Blough, N. V.: Optical absorption and fluorescence properties of chromophoric dissolved organic matter in natural waters, Limnol. Oceanogr., 39, 1903–1916, 1994.
Guéguen, C., Granskog, M. A., McCullough, G., and Barber, D. G.: Characterisation of colored dissolved organic matter in Hudson Bay and Hudson Strait using parallel factor analysis, J. Marine Syst., 88, 423–433, 2011.
Häder, D.-P., Kumar, H. D., Smith, R. C., and Worrest, R. C.: Effects on aquatic ecosystems, J. Photoch. Photobio. B, 46, 53–68, 1998.
Hasegawa, T., Kasai, H., Ono, T., Tsuda, A., and Ogawa, H.: Dynamics of dissolved and particulate organic matter during the spring bloom in the Oyashio region of the western subarctic Pacific Ocean, Aquat. Microb. Ecol., 60, 127–138, 2010.
Helms, J. R., Stubbins, A., Ritchie, J. D., Minor, E. C., Kieber, D. J., and Mopper, K.: Absorption spectral slopes and slope ratios as indicators of molecular weight, source, and photobleaching of chromophoric dissolved organic matter, Limnol. Oceanogr., 53, 955–969, 2008.
Herndl, G. J., Muller-Niklas, G., and Frick, J.: Major role of ultraviolet-B in controlling bacterioplankton growth in the surface layer of the ocean, Cah. Rev. The., 361, 717–719, 1993.
Kawai, H.: Hydrography of the Kuroshio Extention, in: Kuroshio, edited by: Stommel, H. and Yoshida, K., University of Tokyo Press, 235–352, 1972.
Kitidis, V., Stubbins, A. P., Uher, G., Goddard, R. C. U., Law, C. S., and Woodward, E. M. S.: Variability of chromophoric organic matter in surface waters of the Atlantic Ocean, Deep-Sea Res. Pt. II, 53, 1666–1684, 2006.

BGD
10, 9989–10019, 2013

Kobari, T., Mitsui, K., Ota, T., Ichinomiya, M., and Gomi, Y.: Response of heterotrophic bacteria to the spring phytoplankton bloom in the Oyashio region, Deep-Sea Res. Pt. II, 57, 1671–1678, 2010.

Kudo, I., Noiri, Y., Cochlan, W. P., Suzuki, K., Aramaki, T., Ono, T., and Nojiri, Y.: Primary productivity, bacterial productivity and nitrogen uptake in response to iron enrichment during the SEEDS II, Deep-Sea Res. Pt. II, 56, 2755–2766, 2009.

Matsuoka, A., Huot, Y., Shimada, K., Saitoh, S., and Babin, M.: Bio-optical characteristics of the western Arctic Ocean: implications for ocean color algorithms, Can. J. Remote Sens., 33, 503–518, 2007.

Mladenov, N., Sommaruga, R., Morales-Baquero, R., Laurion, I., Camarero, L., Diéguez, M. C., Camacho, A., Delgado, A., Torres, O., Chen, Z., Felip, M., and Reche, I.: Dust inputs and bacteria influence dissolved organic matter in clear alpine lakes, Nat. Commun., 2, 405, doi:10.1038/ncomms1411, 2011.

Mopper, K. and Kieber, D. J.: Photochemistry and the cycling of carbon, sulfer, nitrogen and phosphorus, in: Biogeochemistry of Marine Dissolved Organic Matter, edited by: Carlson, C. and Hansell, D., Academic Press, 455–508, 2002.

Nelson, N. B. and Siegel, D. A.: Chromophoric DOM in the open ocean, in: Biogeochemistry of Marine Dissolved Organic Matter, edited by: Carlson, C. and Hansell, D., Academic Press, 547–578, 2002.

Nelson, N. B. and Siegel, D. A.: The global distribution and dynamics of chromophoric dissolved organic matter, Annu. Rev. Mar. Sci., 5, 447–476, 2013.

Nelson, N. B., Siegel, D. A., and Michaels, A. F.: Seasonal dynamics of colored dissolved material in the Sargasso Sea, Deep-Sea Res. Pt. I, 45, 931–957, 2002.

Nelson, N. B., Carlson, C. A., and Steinberg, D. K.: Production of chromophoric dissolved organic matter by Sargasso Sea microbes, Mar. Chem., 89, 273–287, 2004.

Nelson, N. B., Siegel, D. A., Carlson, C. A., Swan, C., Smethie Jr., W. M., and Khatiwala, S.: Hydrography of chromophoric dissolved organic matter in the North Atlantic, Deep-Sea Res. Pt. I, 54, 710–731, 2007.

Nelson, N. B., Siegel, D. A., Carlson, C. A., and Swan, C. M.: Tracing global biogeochemical cycles and meridional overturning circulation using chromophoric dissolved organic matter, Geophys. Res. Lett., 37, L03610, doi:10.1029/2009GL042325, 2010.

BGD
10, 9989–10019, 2013

Omori, Y., Hama, T., Ishii, M., and Saito, S.: Relationship between the seasonal change in fluorescent dissolved organic matter and mixed layer depth in the subtropical western North Pacific, J. Geophys. Res., 115, C06001, doi:10.1029/2009JC005526, 2010.
Omori, Y., Hama, T., Ishii, M., and Saito, S.: Vertical change in the composition of marine humic-like fluorescent dissolved organic matter in the subtropical western North Pacific and its relation to photoreactivity, Mar. Chem., 124, 38–47, 2011.
Ortega-Retuerta, E., Frazer, T. K., Duarte, C. M., Ruiz-Halpern, S., Tovar-Sánchez, A., Arrieta, J. M., and Reche, I.: Biogeneration of chromophoric dissolved organic matter by bacteria and krill in the Southern Ocean, Limnol. Oceanogr., 54, 1941–1950, 2009.
Ortega-Retuerta, E., Reche, I., Pulido-Villena, E., Agustí, S., and Duarte, C. M.: Distribution and photoreactivity of chromophoric dissolved organic matter in the Antarctic Peninsula (Southern Ocean), Mar. Chem., 118, 129–139, 2010.
Osburn, C. L., Wigdahl, C. R., Fritz, S. C., and Saros, J. E.: Dissolved organic matter composition and photoreactivity in prairie lakes of the US Great Plains, Limnol. Oceanogr., 56, 2371–2390, 2011.
Romera-Castillo, C., Álvarez-Salgado, X., Galí, M., Gasol, J. M., and Marrasé, C.: Combined effect of light exposure and microbial activity on distinct dissolved organic matter pools. A seasonal field study in an oligotrophic coastal system (Blanes Bay, NW Mediterranean), Mar. Chem., 148, 44–51, 2013.
Saito, H., Tsuda, A., and Kasai, H.: Nutrient and plankton dynamics in the Oyashio region of the western subarctic Pacific Ocean, Deep-Sea Res. Pt. II, 49, 5463–5486, 2002.
Sasaki, H, Siswanto, E., Nishiuchi, K., Tanaka, K., Hasegawa, T., and Ishizaka, J.: Mapping the low salinity Changjiang Diluted Water using satellite-retrieved colored dissolved organic matter (CDOM) in the East China Sea during high river flow season, Geophys. Res. Lett., 35, L04604, doi:10.1029/2007GL032637, 2004.
Shank, C. G. and Evans, A.: Distribution and photoreactivity of chromophoric dissolved organic matter in northern Gulf of Mexico shelf waters, Cont. Shelf Res., 31, 1128–1139, 2011.
Shank, C. G., Lee, R., Vähätalo, A., Zepp, R. G., and Bartels, E.: Production of chromophoric dissolved organic matter from mangrove leaf litter and floating Sargassum colonies, Mar. Chem., 119, 172–181, 2010.
Siegel, D. A., Maritorena, S., Nelson, N. B., Hansell, D. A., and Lorenzi-Kayser, M.: Global distribution and dynamics of colored dissolved and detrital organic materials, J. Geophys. Res., 107, C123228, doi:10.1029/2001JC000965, 2002.

BGD
10, 9989–10019, 2013

Smith, R. C., Prezelin, B. B., Baker, K. S., Bidigare, R. R., Boucher, N. P., Coley, T., Karentz, D., MacIntyre, S., Matlick, H. A., Menzies, D., Ondrusek, M., Wan, Z., and Waters, K. J.: Ozone depletion: ultraviolet radiation and phytoplankton biology in Antarctic waters, Science, 255, 952–959, 1992.

Spencer, R. G. M., Butler, K. D., and Aiken, G. R.: Dissolved organic carbon and chromophoric dissolved organic matter properties of rivers in the USA, J. Geophys. Res., 117, G03001, doi:10.1029/2011JG001928, 2012.

Stedmon, C. A., Markager, S., and Kaas, H.: Optical properties and signatures of chromophoric dissolved organic matter (CDOM) in Danish coastal waters, Estuar. Coast. Shelf S., 51, 267–278, 2000.

Steinberg, D. K., Nelson, N. B., Carlson, C. A., and Prusak, A. C.: Production of chromophoric dissolved organic matter (CDOM) in the open ocean by zooplankton and the colonial cyanobacterium *Trichodesmium spp*, Mar. Ecol. Prog. Ser., 267, 45–56, 2004.

Stubbins, A., Niggemann, J., and Dittmar, T.: Photo-lability of deep ocean dissolved black carbon, Biogeosciences, 9, 1661–1670, doi:10.5194/bg-9-1661-2012, 2012.

Suga, T., Motoki, K., and Aoki, Y.: The North Pacific climatology of winter mixed layer and mode waters, J. Phys. Oceanogr., 34, 3–22, 2004.

Swan, C. M., Siegel, D. A., Nelson, N. B., Carlson, C. A., and Nasir, E.: Biogeochemical and hydrographic controls on chromophoric dissolved organic matter distribution in the Pacific Ocean, Deep-Sea Res. Pt. I, 56, 2175–2192, 2009.

Swan, C. M., Nelson, N. B., Siegel, D. A., and Kostadinov, T. S.: The effect of surface irradiance on the absorption spectrum of chromophoric dissolved organic matter in the global ocean, Deep-Sea Res. Pt. I, 63, 52–64, 2012.

Twardowski, M. S., Boss, E., Sullivan, J. M., and Donaghay, P. L.: Modeling the spectral shape of absorption by chromophoric dissolved organic matter, Mar. Chem., 89, 69–88, 2004.

Vernet, M. and Whitehead, K.: Release of ultraviolet-absorbing compounds by the red-tide dinoflagellate Lingulodinium polyedra, Mar. Biol., 127, 35–44, 1996.

Welschmeyer, N. A.: Fluorometric analysis of chlorophyll *a* in the presence of chlorophyll *b* and phaeopigments, Limnol. Oceanogr., 39, 1985–1992, 1994.

Yamashita, Y. and Tanoue, E.: In situ production of chromophoric dissolved organic matter in coastal environments, Geophys. Res. Lett., 31, L14302, doi:10.1029/2004GL019734, 2004.

Yamashita, Y. and Tanoue, E.: Production of bio-refractory fluorescent dissolved organic matter in the ocean interior, Nat. Geosci., 1, 579–582, 2008.

BGD
10, 9989–10019, 2013

Yamashita, Y. and Tanoue, E.: Basin scale distribution of chromophoric dissolved organic matter in the Pacific Ocean, Limnol. Oceanogr., 54, 598–609, 2009.
Yamashita, Y., Maie, N., Briceño, H., and Jaffé R.: Optical characterization of dissolved organic matter in tropical rivers of the Guayana Shield, Venezuela, J. Geophys. Res., 115, G00F10, doi:10.1029/2009JG000987, 2010a.
Yamashita, Y., Scinto, L., Maie, N., and Jaffé, R.: Dissolved organic matter characteristics across a subtropical wetland's landscape: application of optical properties in the assessment of environmental dynamics, Ecosystems, 13, 1006–1019, 2010b.
Zhang, Y., van Dijk, M. A., Liu, M., Zhu, G., and Qin, B.: The contribution of phytoplankton degradation to chromophoric dissolved organic matter (CDOM) in eutrophic shallow lakes: field and experimental evidence, Water Res., 43, 4685–4697, 2009a.
Zhang, Y., Liu, M., Qin, B., and Feng, S.: Photochemical degradation of chromophoric-dissolved organic matter exposed to simulated UV-B and natural solar radiation, Hydrobiologia, 627, 159–168, 2009b.

BGD
10, 9989–10019, 2013

Table 1. Sample details for dark microbial incubations and photo-irradiation experiments.

Experiment	Type	Location	Depth (m)	Temp. (°C)	Salinity	Chl *a* ($\mu g L^{-1}$)	a_{320} (m^{-1})	$S_{275-295}$ (nm^{-1})	$S_{350-400}$ (nm^{-1})	S_R
SAM-1	Microbial incubation	41.7° N, 144.0° E	5	4.5	32.88	1.22	0.284	0.0303	0.0141	2.15
SAM-2	Microbial incubation	41.5° N, 144.0° E	5	4.4	32.99	2.06	0.398	0.0279	0.0136	2.05
STP-1	Photo-irradiation	29.0° N, 129.0° E	400	14.3	34.52	–	0.158	0.0294	0.0134	2.20
STP-2	Photo-irradiation	29.0° N, 129.0° E	766	5.7	34.35	–	0.216	0.0216	0.0127	1.70

BGD
10, 9989–10019, 2013

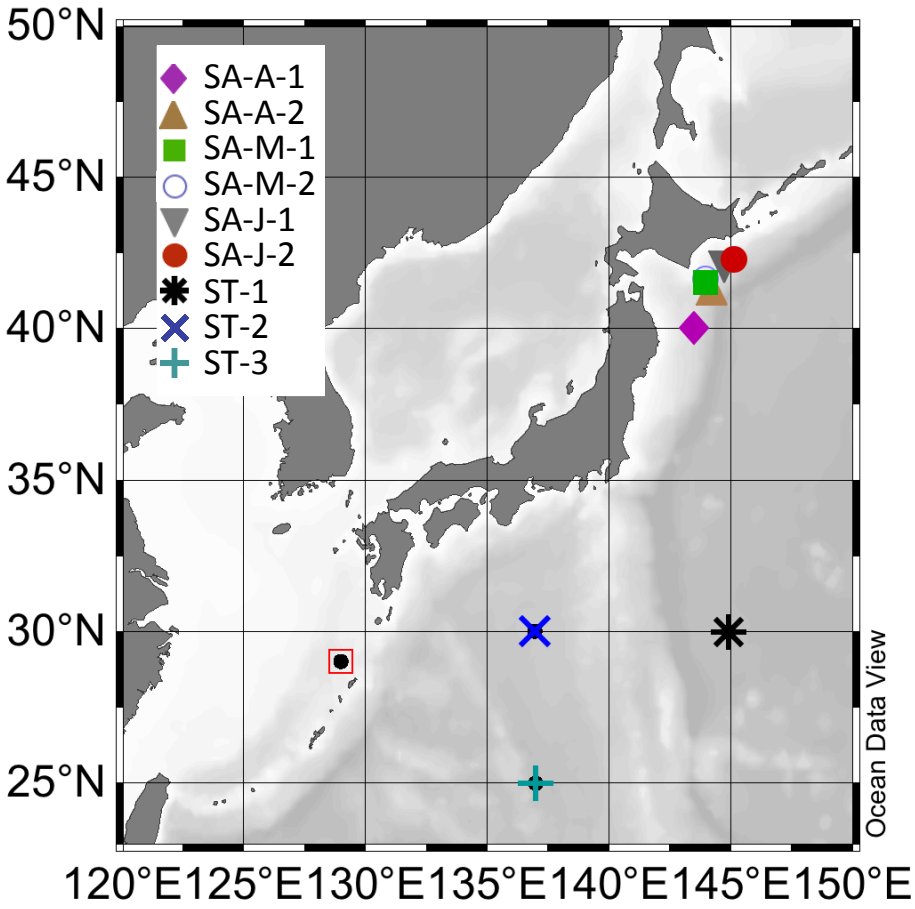

Fig. 1. Sampling locations. Samples for photo-irradiation experiments were collected from the station located at 29.0° N, 129.0° E (STP).

BGD
10, 9989–10019, 2013

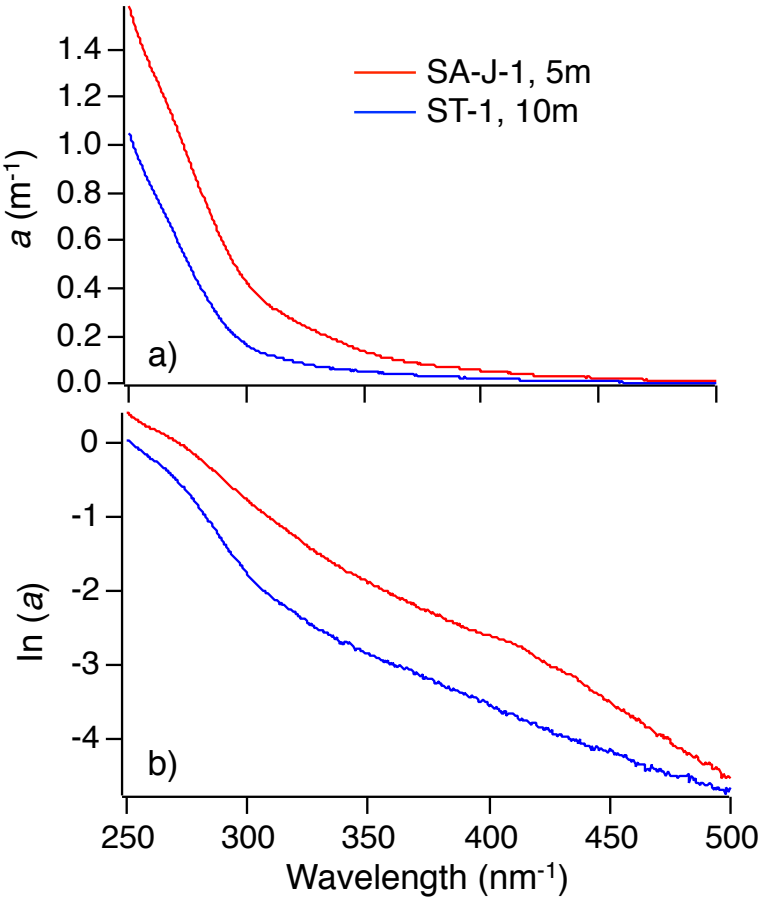

Fig. 2. Typical absorption spectrum at the subarctic (SA-J-1, 5 m) and the subtropical (ST-1, 10 m) regions: **(a)** on linear scale and **(b)** on logarithmic scale.

BGD
10, 9989–10019, 2013

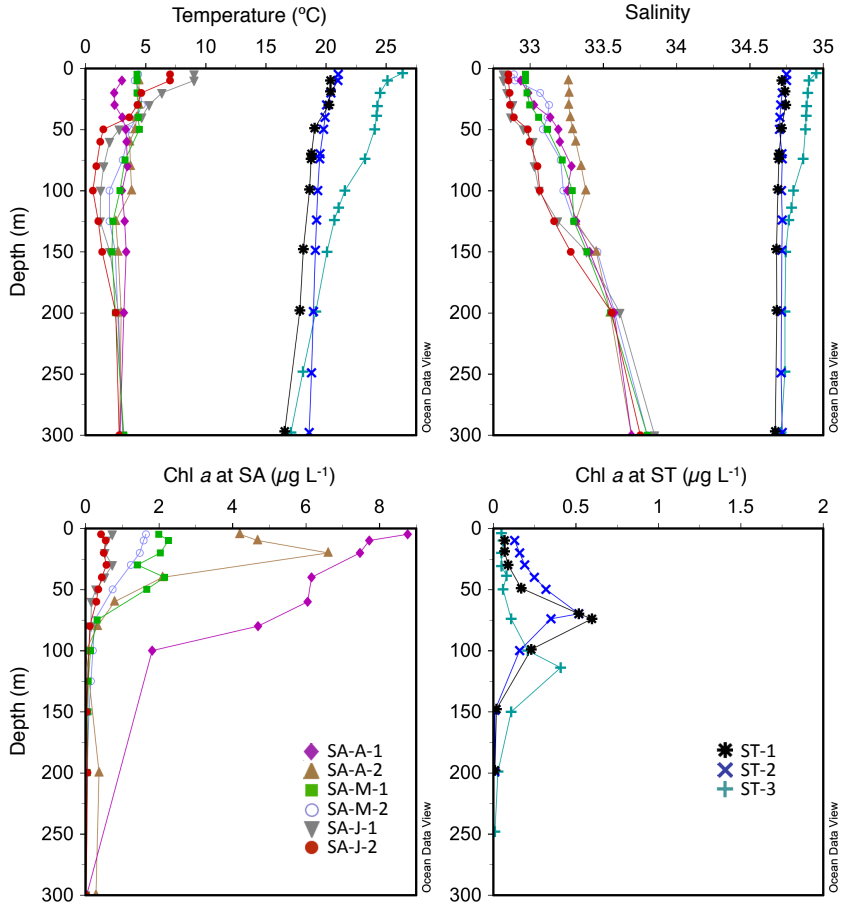

Fig. 3. Vertical profiles of temperature, salinity, and chlorophyll *a* concentration at the subarctic region (SA) and the subtropical region (ST). Note: ranges of X-axis for chlorophyll *a* concentration were different between SA and ST.

BGD
10, 9989–10019, 2013

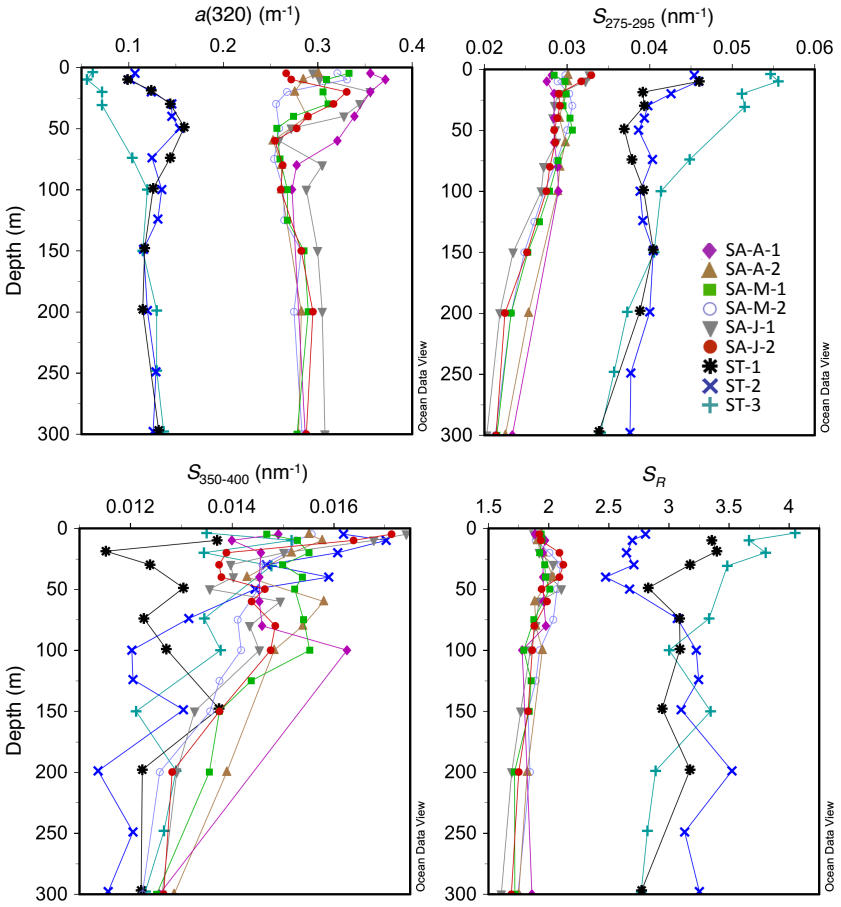

Fig. 4. Vertical profiles of $a(320)$, $S_{275–295}$, $S_{350–400}$, and S_R at the subarctic and subtropical regions.

BGD
10, 9989–10019, 2013

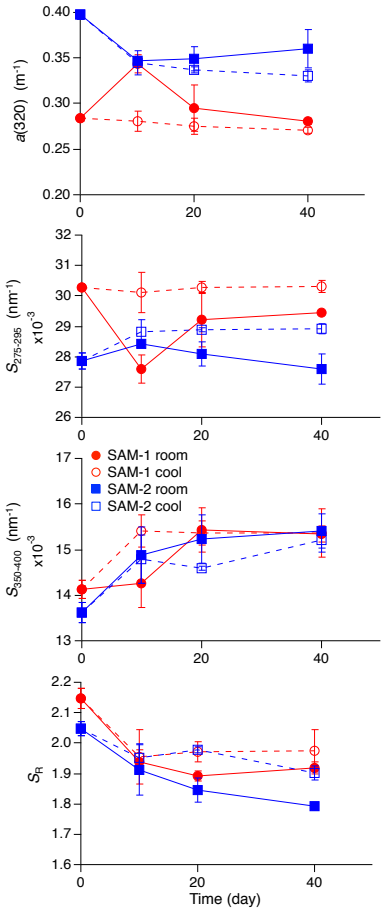

Fig. 5. Changes in $a(320)$, $S_{275–295}$, $S_{350–400}$, and S_R during dark microbial incubation experiments of the subarctic surface waters for 40 days.

BGD
10, 9989–10019, 2013

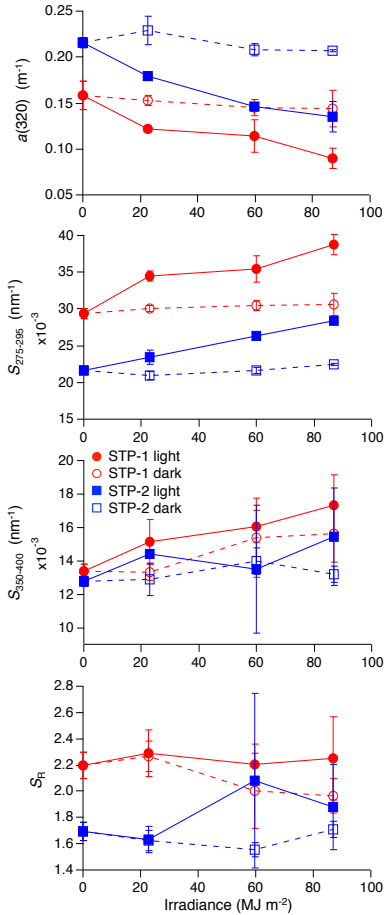

Fig. 6. Changes in $a(320)$, $S_{275–295}$, $S_{350–400}$, and S_R during photo-irradiation experiments of the subtropical deep waters. Note: 23, 60, and 87 MJ m^{-2} on the X-axis was corresponding to 2, 6, and 13 days for the dark control experiments, respectively.

BGD
10, 9989–10019, 2013